Photoacoustic Imaging with Augmented Reality for Surgical Guidance

Junhao Zhang[1*], Cynthia Li[1,2], and Muyinatu A. Lediju Bell[1,3,4*]

[1]Johns Hopkins University, Department of Electrical & Computer Engineering, Baltimore, MD, USA
[2]Massachusetts Institute of Technology, Department of Electrical Engineering and Computer Science, Cambridge, MA, USA
[3]Johns Hopkins University, Department of Biomedical Engineering, Baltimore, MD, USA
[4]Johns Hopkins University, Department of Computer Science, Baltimore, MD, USA

ABSTRACT

Photoacoustic-guided surgery benefits from precise co-alignment between the light delivery and sound reception device components. Misalignment can result in absent photoacoustic signals, potentially leading to critical structures incorrectly interpreted as absent. Augmented reality has the potential to provide real-time spatial registration and intuitive visualization through tracking of the laser and ultrasound transducer positions. We developed and validated a novel augmented reality guidance system that tracks the laser source and ultrasound transducer, rendering real-time virtual representations of the associated laser beam and ultrasound image to facilitate intuitive alignment. Quantitative evaluation using a submerged hex key target demonstrated a 58% reduction in mean targeting error during static alignment tasks, relative to a standard freehand approach implemented without augmented reality. Results indicate that augmented reality as a promising approach to address anticipated challenges surrounding freehand photoacoustic-guided surgery.

Keywords: Augmented reality, virtual reality, photoacoustic imaging, surgical guidance *

1. INTRODUCTION

Photoacoustic imaging is a promising biomedical modality that combines the high contrast of optical imaging with the deep tissue penetration of ultrasound.[1] By exciting tissue with short-pulsed, non-ionizing laser light and detecting the resulting ultrasonic waves, photoacoustic imaging can map hemoglobin concentration, lipid distribution, and other chromophores in real time with greater contrast than traditional ultrasound.[2–5] This capability makes photoacoustic imaging particularly valuable for surgical guidance by identifying critical structures such as blood vessels, nerves, and tumors.[6–9]

When photoacoustic imaging is used to guide surgeries, light sources may be attached to surgical tools[10–12] or undergo freehand operation[13,14] to make decisions about the location of critical structures hidden by tissue.[15,16] However, the independence of light delivery from an ultrasound transducer introduces an alignment challenge. In particular, the laser path must intersect the two-dimensional image plane of the ultrasound transducer to generate detectable photoacoustic signals. Misalignment can result in no photoacoustic signals, leading to an incorrect conclusion that there are no critical structures in view, when in reality the existing structure, light profile, and image plane are misaligned.[15,16] Alignment can be performed manually, requiring surgeons and interventionalists to make fine adjustments based on visual feedback from an external monitor, which demands considerable expertise and requires additional time during surgical procedures.[17]

Beyond alignment challenges, widespread adoption of photoacoustic imaging is limited by difficulties in image interpretation and spatial registration. Traditional systems present 2D images on external monitors that require expertise to mentally map to anatomical structures, which can present a distraction during procedures.[17] Without additional guidance, surgeons may need to shift attention from the patient to the image display monitor or ultrasound transducer position, which would increase cognitive load and the potential for errors.

*Address correspondence to: jzhan363@jh.edu and mledijubell@jhu.edu

Photons Plus Ultrasound: Imaging and Sensing 2026, edited by Alexander A. Oraevsky, Lihong V. Wang,
Proc. of SPIE Vol. PC13851, PC138511R · 2026 Published by SPIE · 1605-7422 · doi: 10.1117/12.3084555

Augmented reality technology offers a compelling solution to surgical guidance challenges by overlaying virtual information onto the physical world viewed by the user.[18] These virtual counterparts to the physical world can be rendered in the original position of objects in the physical world by tracking the positions of the laser and ultrasound transducer, thereby transforming the alignment task from challenging to intuitive.[19] Augmented reality can also be employed to overlay photoacoustic data on the anatomy of a patient, thereby improving spatial understanding and reducing the cognitive burden of mental registration. While augmented reality has been successfully applied to other medical imaging domains, such as ultrasound-guided procedures[18,20] and computed tomography,[21] its integration with photoacoustic imaging is limited. Previous work by Suzuki *et al.*[22] demonstrated a method to overlay preexisting photoacoustic images onto anatomical structures for preoperative visualization. However, this approach required preoperative photoacoustic images and did not address the fundamental challenge of real-time transducer alignment during image acquisition.

Herein, we investigate real-time augmented reality guidance for the initial alignment process of the photoacoustic system, enabling users to efficiently position the laser and ultrasound transducer to obtain photoacoustic images of targeted structures in real-time. We present the design, implementation, and initial evaluation of our novel augmented reality-guided photoacoustic imaging system, which renders a geometrically calibrated model of the laser beam and overlays a live video feed of the photoacoustic image onto a virtual imaging plane. These innovations are designed to assist with real-time spatial registration and visualization by providing reliable image overlays and intuitive image guidance for users.

2. MATERIALS AND METHODS

2.1 System Architecture

Three major design components of our system include: (1) physical markers for the surgical tools, (2) a Unity application (Unity Technologies, San Francisco, CA, USA) for the Magic Leap 2 headset (Magic Leap Inc., Plantation, FL, USA) to perform tracking and rendering, and (3) a calibration protocol to ensure the geometric accuracy of the virtual laser beam. The hardware component of our system was designed to track a handheld laser source (Vevo F2, FUJIFILM VisualSonics Inc., Toronto, ON, Canada) and ultrasound transducer (UHF29x, FUJIFILM VisualSonics Inc., Toronto, ON, Canada). Custom holders were designed using Autodesk Fusion 360 (Autodesk Inc., San Francisco, CA, USA) to affix ArUco fiducial markers to each device. Our laser holder design incorporated two modular pyramid structures with 20 mm square ArUco markers positioned at 45-degree angles relative to the base, as shown in Fig. 1.

2.2 Marker Detection and Pose Estimation

Tracking software was developed using a Unity application with custom C# scripts running on the Magic Leap 2 augmented reality platform. Markers were detected through front-facing cameras on the Magic Leap 2 headset. Upon marker detection, an API provided unique marker IDs and associated poses with 6 degrees of freedom (DOF) in the world coordinate system. To determine the device positions and orientations in the world coordinate system after detecting the markers, spatial transformations from the marker origin to the device were computed from 3D models of the device scanned and reconstructed using Polycam software (Polycam Inc., San Francisco, CA, USA). When multiple markers were detected on a single device, the Unity application calculated individual pose candidates by applying stored offsets to the world pose of each marker. To generate a single, stable device pose, the vectors of candidate positions and rotations were averaged using quaternion interpolation.

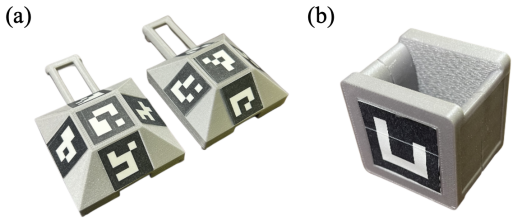

Figure 1: Marker holder for the (a) laser source and (b) ultrasound probe.

The averaged pose of the laser beam origin was applied to the virtual counterpart to the physical laser. To mitigate flickering due to transient tracking loss, a 0.1-second buffer was applied, maintaining the virtual object at its last known pose when markers were temporarily undetected. To ensure stable visualization of the image plane, the ultrasound transducer was fixed in place, which is consistent with a configuration reported in previous photoacoustic guidance systems.[11,23–25]

2.3 Visualization and Interaction

To render the virtual image plane, a Unity quad object with dimensions of 23.35 mm × 23.0 mm, matching the imaging area of the ultrasound transducer, was created at the beginning of the Unity application. On a server computer running a custom Python script and connected to the photoacoustic imaging system, each photoacoustic image frame was compressed using the Deflate algorithm.[26] The resulting compressed byte stream was then preceded by a 4-byte header indicating its length before being trasnmitted over TCP to the augmented reality client.

To render the virtual laser beam, the LineRenderer component of the Unity software was utilized. A dynamic elliptical visual element represented the virtual laser beam intersection with the virtual photoacoustic imaging plane. Laser-plane intersection was detected using the raycast system of the Unity software. When this intersection occurred, the elliptical visual element, positioned at the intersection point, provided visual feedback for laser-transducer alignment.

The two rendering threads occurred concurrently with data reception on the augmented reality headset. In particular, a dedicated data reception thread was employed to asynchronously perform data reception, header parsing, frame extraction, then decompression, followed by buffering, to ensure smooth real-time rendering in Unity. The concurrent data reception and rendering multithread operations prevented network and decompression operations from blocking the Unity main rendering thread, thereby allowing continuous frame updates and smooth rendering performance. After decompression, each frame was stored in a buffer queue to minimize latency and limit memory buildup. Each frame was converted into a Texture2D object (640×480, RGB24) and updated at a rate of 30 Hz for real-time display, which ocurred asynchronously from the data reception thread.

2.4 Targeting Evaluation Tasks

A hex key submerged in water was used in the photoacoustic imaging setup (Fig. 2(a)). The position of the hex key was adjusted to the image center according to the co-registered ultrasound image (Fig. 2(b)). With the guidance of augmented reality, the operator was asked to align the laser path to intersect the hex key (Fig. 2(c)).

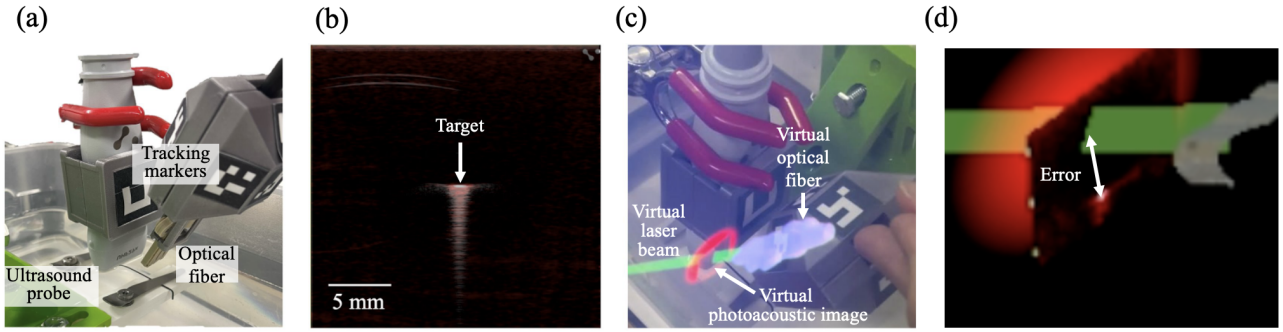

Figure 2: (a) Experimental setup with fixed ultrasound transducer and handheld laser, each tracked with custom ArUco markers. (b) Co-registered photoacoustic and ultrasound images displaying target signal at the imaging plane center. (c) Augmented reality user view showing virtual laser beam (green) intersecting virtual image plane (red) with live photoacoustic image overlay. (d) Demonstration of the error calculation, defined as the Euclidean distance between the intersection of the virtual laser with the virtual image plane and the center of the virtual image plane.

The operator was also asked to perform the alignment task while looking at the photoacoustic image without using the augmented reality device. During these tasks, the server computer recorded the laser-plane intersection coordinates on the virtual image plane at a frame rate of 1 Hz as the laser source was maintained at the image plane center during three-minute time intervals with and without the augmented reality device. Considering that optimal photoacoustic signal generation occurred when the center of the laser beam intersects the center of the ultrasound imaging plane (where the hex key target was located), accurate alignment was defined as coincidence among the hex key signal, the virtual laser center, and the center of the virtual photoacoustic image plane. The Euclidean distance between the virtual laser intersection point and the center of the virtual photoacoustic plane illustrated in Fig. 2(d) was then calculated for each image acquired during the three-minute time intervals.

3. RESULTS AND DISCUSSION

Fig. 3 shows the spatial distribution of laser intersection points on the photoacoustic imaging plane (Fig. 3(a)) and the temporal evolution of the targeting errors (Fig. 3(b)) with (blue) and without (red) augmented reality. With augmented reality, the user did not rely on access to the Vevo F2 external monitor. Without augmented reality assistance, the user relied solely on the Vevo F2 external monitor for visual feedback, resulting in greater deviations from the target center. The mean targeting error with augmented reality assistance was 3.31 mm (standard deviation: 1.81 mm), compared to 7.88 mm (standard deviation: 3.31 mm) without augmented reality guidance, representing a 58% reduction in mean targeting error when using the augmented reality system. Considering that photons can reach targets located outside the direct laser beam path due to tissue scattering, a tracking accuracy of 3.31 mm is consindered acceptable.

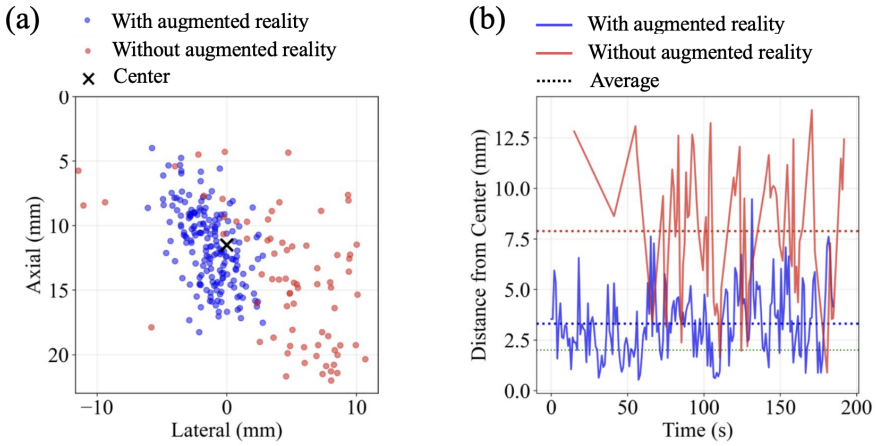

Figure 3: (a) Spatial distribution of laser intersection points on the photoacoustic image plane while attempting to target the image plane center (x) with (blue) and without (red) augmented reality guidance. (b) Temporal evolution of distances between laser intersection positions and imaging plane center, with the average distances indicated by dashed lines.

4. CONCLUSION

This paper presents the first known augmented reality photoacoustic image guidance system, intended to improve real-time laser-transducer alignment. This system reduces targeting errors by 58% relative to traditional monitor-based alignment. Our initial results demonstrate the feasibility of augmented reality as a promising approach to address usability challenges that have limited the adoption of photoacoustic-guided surgery with light sources separated from acoustic receivers.

Acknowledgments

This work is supported by the Chan Zuckerberg Initiative DAF (an advised fund of the Silicon Valley Community Foundation) (Grant No. 2022-309513), the National Institutes of Health (NIH) (Grant No. R01 EB032358),

and the National Science Foundation (NSF) Alan T. Waterman Award (Grant No. IIS-2431810). This work was also completed in partnership with the NSF Computational Sensing and Medical Robotics Research Experience for Undergraduates program (Grant No. EEC-1852155).

REFERENCES

[1] Beard, P., "Biomedical photoacoustic imaging," *Interface Focus* **1**, 602–631 (Aug. 2011).

[2] González, E. A. and Bell, M. A. L., "Dual-wavelength photoacoustic atlas method to estimate fractional methylene blue and hemoglobin contents," *Journal of Biomedical Optics* **27**(9), 096002 (2022).

[3] Sangha, G. S., Phillips, E. H., and Goergen, C. J., "In vivo photoacoustic lipid imaging in mice using the second near-infrared window," *Biomedical optics express* **8**(2), 736–742 (2017).

[4] Park, E., Lee, Y.-J., Lee, C., and Eom, T. J., "Effective photoacoustic absorption spectrum for collagen-based tissue imaging," *Journal of biomedical optics* **25**(5), 056002–056002 (2020).

[5] Shi, J., Wong, T. T., He, Y., Li, L., Zhang, R., Yung, C. S., Hwang, J., Maslov, K., and Wang, L. V., "High-resolution, high-contrast mid-infrared imaging of fresh biological samples with ultraviolet-localized photoacoustic microscopy," *Nature photonics* **13**(9), 609–615 (2019).

[6] Graham, M. T., Sharma, A., Padovano, W. M., Suresh, V., Chiu, A., Thon, S. M., Tuffaha, S., and Bell, M. A. L., "Optical absorption spectra and corresponding in vivo photoacoustic visualization of exposed peripheral nerves," *Journal of Biomedical Optics* **28**(9), 097001–097001 (2023).

[7] Kakkar, M., Shahid, M., Shivram, S. P., Suresh, R., Padovano, W., Tuffaha, S., and Bell, M. A. L., "A multispectral photoacoustic imaging approach to detect nerve injury during surgery," in [*2025 IEEE International Ultrasonics Symposium (IUS)*], 1–4, IEEE (2025).

[8] Kempski, K. M., Wiacek, A., Graham, M., González, E., Goodson, B., Allman, D., Palmer, J., Hou, H., Beck, S., He, J., and Bell, M. A. L., "In vivo photoacoustic imaging of major blood vessels in the pancreas and liver during surgery," *Journal of Biomedical Optics* **24**(12), 121905 (2019).

[9] Zhang, J., Arroyo, J., and Lediju Bell, M. A., "Multispectral photoacoustic imaging of breast cancer tissue with histopathology validation," *Biomedical Optics Express* **16**(3), 995–1005 (2025).

[10] Gandhi, N., Allard, M., Kim, S., Kazanzides, P., and Bell, M. A. L., "Photoacoustic-based approach to surgical guidance performed with and without a da Vinci robot," *Journal of Biomedical Optics* **22**(12), 121606 (2017).

[11] Eddins, B. and Bell, M. A. L., "Design of a multifiber light delivery system for photoacoustic-guided surgery," *Journal of Biomedical Optics* **22**(4), 041011 (2017).

[12] Gao, S., Jiang, Y., Li, M., Wang, Y., Shen, Y., Flegal, M. C., Nephew, B. C., Fischer, G. S., Liu, Y., Fichera, L., et al., "Laparoscopic photoacoustic imaging system based on side-illumination diffusing fibers," *IEEE Transactions on Biomedical Engineering* **70**(11), 3187–3196 (2023).

[13] Bell, M. A. L., Kuo, N. P., Song, D. Y., Kang, J. U., and Boctor, E. M., "In vivo visualization of prostate brachytherapy seeds with photoacoustic imaging," *Journal of Biomedical Optics* **19**(12), 126011 (2014).

[14] Mitcham, T., Dextraze, K., Taghavi, H., Melancon, M., and Bouchard, R., "Photoacoustic imaging driven by an interstitial irradiation source," *Photoacoustics* **3**(2), 45–54 (2015).

[15] Bell, M. A. L., "Photoacoustic imaging for surgical guidance: principles, applications, and outlook," *Journal of Applied Physics* **128**(6), 060904 (2020).

[16] Wiacek, A. and Bell, M. A. L., "Photoacoustic-guided surgery from head to toe," *Biomedical Optics Express* **12**(4), 2079–2117 (2021).

[17] Peng, C., Cai, Q., Chen, M., and Jiang, X., "Recent advances in tracking devices for biomedical ultrasound imaging applications," *Micromachines* **13**(11) (2022).

[18] Zhang, J. and Bell, M. A. L., "Maximizing the accuracy of ultrasound imaging with augmented reality," in [*2025 IEEE International Ultrasonics Symposium (IUS)*], 1–4, IEEE (2025).

[19] Shuhaiber, J. H., "Augmented reality in surgery," *Arch. Surg.* **139**, 170–174 (Feb. 2004).

[20] Nguyen, T., Plishker, W., Matisoff, A., Sharma, K., and Shekhar, R., "Holous: Augmented reality visualization of live ultrasound images using hololens for ultrasound-guided procedures," *International Journal of Computer Assisted Radiology and Surgery* **17** (11 2021).

[21] Sun, Q., Mai, Y., Yang, R., Ji, T., Jiang, X., and Chen, X., "Fast and accurate online calibration of optical see-through head-mounted display for ar-based surgical navigation using microsoft hololens," *International journal of computer assisted radiology and surgery* **15**(11), 1907–1919 (2020).

[22] Suzuki, Y., Kajita, H., Watanabe, S., Otaki, M., Okabe, K., Sakuma, H., Takatsume, Y., Imanishi, N., Aiso, S., and Kishi, K., "Surgical applications of lymphatic vessel visualization using photoacoustic imaging and augmented reality," *Journal of Clinical Medicine* **11**(1) (2022).

[23] Wiacek, A., Wang, K. C., Wu, H., and Bell, M. A. L., "Photoacoustic-guided laparoscopic and open hysterectomy procedures demonstrated with human cadavers," *IEEE Transactions on Medical Imaging* **40**(12), 3279–3292 (2021).

[24] Bell, M. A. L., Ostrowski, A. K., Li, K., Kazanzides, P., and Boctor, E. M., "Localization of transcranial targets for photoacoustic-guided endonasal surgeries," *Photoacoustics* **3**(2), 78–87 (2015).

[25] Graham, M. T., Huang, J., Creighton, F. X., and Bell, M. A. L., "Simulations and human cadaver head studies to identify optimal acoustic receiver locations for minimally invasive photoacoustic-guided neurosurgery," *Photoacoustics* **19**, 100183 (2020).

[26] Oswal, S., Singh, A., and Kumari, K., "Deflate compression algorithm," *International Journal of Engineering Research and General Science* **4**(1), 430–436 (2016).